Journal of
Mechanics of
Materials and Structures

A CONTRIBUTION TO A CRITICAL REVIEW OF FRICTION STIR WELDING NUMERICAL SIMULATION

Olivier Lorrain, Jérôme Serri, Véronique Favier, Hamid Zahrouni and Mourad El Hadrouz

Volume 4, Nº 2 February 2009

mathematical sciences publishers

JOURNAL OF MECHANICS OF MATERIALS AND STRUCTURES
Vol. 4, No. 2, 2009

A CONTRIBUTION TO A CRITICAL REVIEW OF FRICTION STIR WELDING NUMERICAL SIMULATION

OLIVIER LORRAIN, JÉRÔME SERRI, VÉRONIQUE FAVIER,
HAMID ZAHROUNI AND MOURAD EL HADROUZ

Various modelling approaches using commercial numerical software have been proposed in the friction stir welding literature. We initiate a comparative analysis of such modellings, involving aspects such as the constitutive laws, the representation of the continuum medium and the contact between medium and tool, and the definition of the heat sources. Numerical problems are also considered: contact definition, mass scaling, and the use of the arbitrary Lagrangian Eulerian in ABAQUS/Explicit. Finally, we propose numerical tests to explore the ability of a Lagrangian code with an ALE option to simulate the process.

1. Introduction

Friction stir welding (FSW) is a process developed by The Welding Institute in the early 1990s. Its principle is simple: a rotating tool is plunged into the weld joint and is forced to translate along the joint line between two pieces of plate material which are butted together. The tool is made of two parts: a shoulder, which heats the sheet by friction (allowing the material to soften) and prevents the outflow of material due to the compressive effort, and a pin, which stirs the material to avoid holes and makes a compacts joint. The process is thus a combination of extruding, forging, and stirring. Figure 1 illustrates a weld in a 7020-T6 aluminium alloy.

The specific strengths of the process lie in the joining of the material without melting and the consequent ability to join hard-to-weld metals such as aluminium alloys, steel-aluminium, or copper-aluminium couples. FSW is used for applications where the original metal characteristics must remain unchanged as far as possible. Another advantage is that the weld can be made in all positions because no welding pool is needed. However, the process requires a very rigid clamping on the backing bar to prevent the abutting joint faces from being forced apart. In addition, the keyhole at the end of the weld can also be considered a drawback.

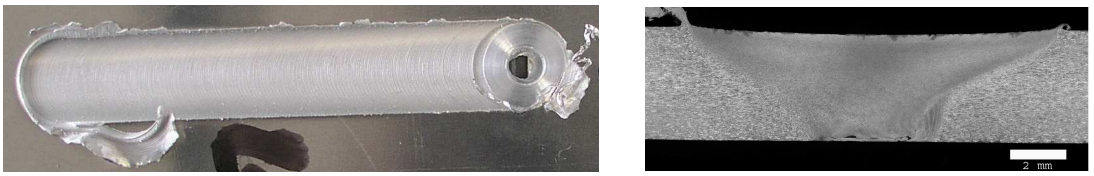

Figure 1. Top view of the weld (left) and cut orthogonal to the welding direction (right).

Keywords: friction stir welding, numerical simulation, finite element.
The authors acknowledge financial and experimental support from the Institut de Soudure and financial support from the Conseil Régional de Lorraine.

Objectives of the study. The thermomechanical conditions of FSW are very hard to determine experimentally. The profile of the pin influences the process directly, as do weld parameters such as the forging force applied to the tool and the rotational and feed speeds [Mishra and Ma 2005].

In order to optimize welding conditions for a given material and plate thickness, a lot of tests and metallurgical and mechanical characterisations of the welded joint have to be performed. Finite element method (FEM) simulations are widely used to obtain temperature and mechanical fields and to optimize the process, lowering development costs. They provide a better understanding of the flow and heating mechanisms of FSW.

A small but increasing number of papers dealing with FSW simulation have appeared in the literature. Such simulations require the modelling of friction, mechanical and thermal behaviour, and kinematics; they must also solve all the field equations. Though the mathematical laws are generally spelled out, their implementation and the numerical treatment of the differential equations are often not clearly explained.

Figure 2 offers a schematic view of inputs, outputs, and defining constraints involved in a numerical model. The inputs, on the left, consist of geometry, process parameters, and material grade. The outputs, on the right, are the mechanical and temperature fields. The choices required for the model are shown above the box.

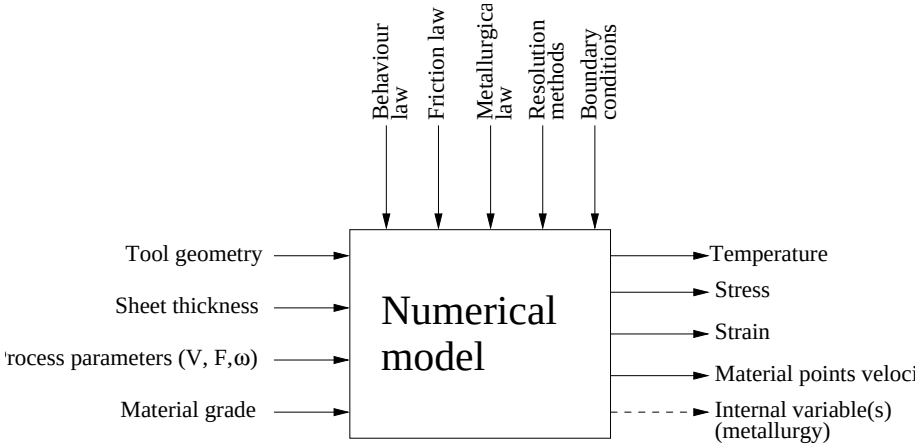

Figure 2. Schematic view of a numerical model.

This article highlights the points that require attention in FSW numerical simulations: mechanical formulation, handling of contact, boundary conditions, and constitutive laws. It also illustrates the influence of numerical parameters on the solution of the contact and field equations.

For the numerical simulation, we consider the finite element code ABAQUS/Explicit, which uses the Lagrangian formulation and offers adaptive meshing. The explicit scheme is well adapted to the building of process simulations.

Section 2 presents a state of the art modelling of the FSW process, consisting of the mechanical formulation, the heat source model, and the physical model. Section 3 discusses numerical issues concerning contact management, mass scaling, and adaptive meshing. A numerical analysis is proposed concerning FSW simulation and accounting for some aspects of the previous discussion.

Problems to be solved. Mechanically and numerically, two different but coupled problems have to be solved in order to provide a realistic computational simulation of the process. The first is the heating of the sheet, which softens the material, making it easy to stir. This heating is governed by the constitutive equation, the friction law, the contact management, thermomechanical coupling, and the boundary conditions (for example, heat exchange between the plates and the surrounding air and the anvil). The second problem is the representation of the kinematics of the flow. The flow undergoes very large deformations and controls the stirring and quality of the welded joint. Its description is therefore a fundamental clue. The challenge in modelling is to provide a numerical tool able to predict the mixing of the materials and the joint defaults.

Both features — large deformations and material stirring — are very difficult to solve numerically using FEM. Computation time is also an obstacle in FSW simulation, especially for industrial uses, and must be kept in mind.

2. Modelling the process

Compared to other joining processes, there are few studies of FSW in the literature, though in the last five years a symposium has been established to bring together different teams and record their work. Most of the papers published are devoted to experimental characterisations of the material created by FSW; only a few deal with computational simulations. This is undoubtedly due to the complexity of the process, which involves mechanical, thermal, and metallurgical phenomena all coupled together.

Mechanical formulations. Finite element simulations require discretization of the continuum medium. The equations of a thermomechanical problem can be written in two different classical formulations: Lagrangian and Eulerian. In the Lagrangian representation, the mesh is attached to material points (also called particles), whereas in the Eulerian representation, the mesh is attached to spatial points. Consequently, during the material flow, in the Lagrangian representation the mesh moves and follows the material points, whereas in the Eulerian representation the mesh is fixed. A mixed representation called the arbitrary Lagrangian Eulerian (ALE), developed to combine the advantages of the two previous ones, allows the mesh to have a different velocity than the material flow.

The Lagrangian representation is the most often used in solid mechanics, where material flow is limited. It consists in describing the movement of the continuum medium compared to a reference configuration. For each particle, which is completely defined by its position at the initial time, the classical equations for the continuum medium provide its current position and associated mechanical fields. Thus the thermomechanical history of each particles is known.

For FSW simulation, this is relevant because the final properties of the joint depend on its metallurgical state, which is strongly affected by the thermomechanical path of the particles [Chen and Kovacevic 2003a; 2003b; Gallais et al. 2004; Buffa et al. 2006b; 2006a; 2007; Fratini et al. 2007]. In addition, deformations, residual stresses, and forces applied on tools can be determined [Chao and Qi 1999; Ulysse 2002; Zhang et al. 2005; Bastier 2006]. However, in FSW, the material is so deformed and distorted that the quality of the mesh decreases during simulations, leading to numerical problems; therefore adaptive meshing (as in ABAQUS [Song and Kovacevic 2003b; 2003a; Schmidt and Hattel 2004; 2005; Zhang et al. 2005; 2007]) or remeshing (as in FORGE2005 [Fourment et al. 2004; Guerdoux and Fourment 2005], for example) is crucial in FSW simulations. In FORGE2005, to limit the size, the mesh is fine

only in a region near the tool. This mesh constraint is attached to the tool. As the tool goes forward, a remeshing is applied after some time increment which allows one to reduce distortions and to follow the tool. An alternative solution is the use of smooth particle hydrodynamics (SPH) [Tartakovsky et al. 2006], which has a Lagrangian particle nature. The material is then represented as particles interacting with each other. Other techniques based on natural element methods (NEM) have also been proposed to model the material flow of the FSW process [Alfaro et al. 2008; 2007].

The Eulerian representation is mainly used in fluid mechanics and consists of observing particles that pass successively through a spatial point. One determines the properties of the particle in terms of time and spatial coordinates. For simulations, the mesh is fixed and the material flows through it. Consequently, this representation does not capture deformations and free surfaces, and additional algorithms are required to introduce free surfaces. In the case of FSW simulations, the Eulerian representation is more appropriate for describing flow because it avoids mesh distortions, especially near the tool [Colegrove et al. 2000; Colegrove et al. 2003; Seidel and Reynolds 2003; Colegrove and Shercliff 2004; Colegrove and Shercliff 2005; 2006; Bastier 2006]. For this Eulerian approach the following commercial software has been used: CASTEM [Bastier 2006], FLUENT [Colegrove et al. 2000; Colegrove et al. 2003; Seidel and Reynolds 2003; Colegrove and Shercliff 2004; Colegrove and Shercliff 2005; 2006], and SYSWELD [Feulvarch et al. 2005a; 2005b; 2007]. However one cannot obtain sheet distortions and residual stresses because the strain history of the material is unknown.

For these reasons, the Eulerian representation is typically used for tool design analysing the material blend as well as the force applied to the tool [Colegrove et al. 2000; Colegrove et al. 2003; Colegrove and Shercliff 2004; Colegrove and Shercliff 2005; 2006], whereas the Lagrangian representation is used when the final microstructure and residual stress are desired. Some authors have used first the Eulerian formulation to obtain the temperature and flow field and then the Lagrangian formulation to compute residual stresses [Bastier 2006].

Another difficulty is determining the zone under study, which has to represent the boundary between "liquid" and "solid" material. The boundary conditions are not easy to estimate, in particular those concerning heat flux between the two parts of the sheet (the part modelled and the part not modelled).

The hybrid ALE method enjoys the advantages of both representations, while avoiding their drawbacks. In this formulation, the mesh changes during the flow but its velocity is different from that of the material, and convective terms appear in the equilibrium equations depending on the difference between the two velocities [Askes and Sluys 2000; Aymone et al. 2001; Gadala et al. 2002; Gadala 2004]. This representation has been used in the last four years to simulate the FSW process, and it seems to provide the most complete modelling. Indeed, the material flow [Xu and Deng 2002; 2003; Fourment et al. 2004; Guerdoux and Fourment 2005], the forces applied on the tool [Schmidt and Hattel 2004; 2005], and the microstructure [Xu and Deng 2003] all seem to be predictable using the ALE formulation.

ABAQUS/Explicit offers this possibility [Schmidt and Hattel 2004; 2005] via the repositioning of nodes in order to decrease mesh distortions. This is a procedure of remeshing of the structure without adding nodes which allows one to obtain elements with acceptable shape. But, even with the use of this formulation, the mixing of the materials is not captured in simulations.

Figure 3, left, presents the year-by-year evolution in the number of scientific papers using one of these three representations since the beginning of FSW modelling. Figure 3, right, shows the overall percentage of use of these representations. The Lagrangian formulation was used earliest. The Eulerian formulation

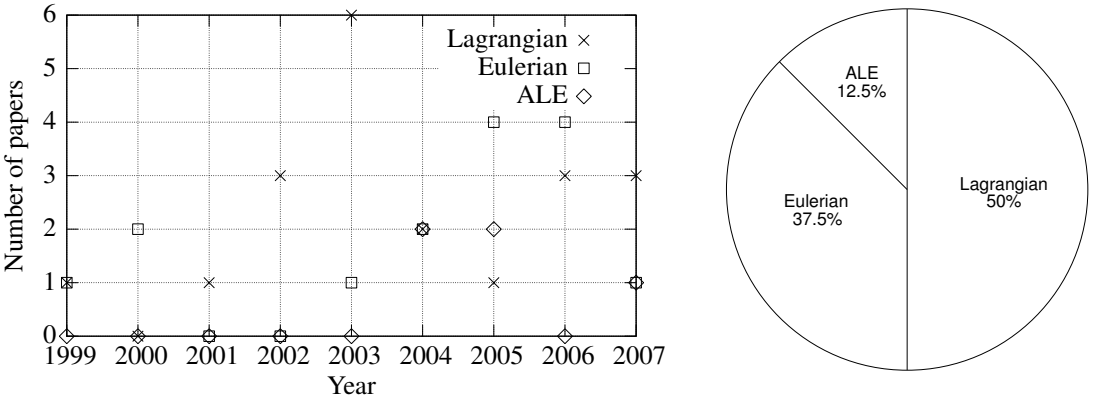

Figure 3. Year-by-year evolution of the mechanical formulation (left) and distribution over the last ten years (right).

was then introduced, perhaps to avoid the problem of excessive mesh distortion and because material flow is a crucial problem that needs to be understood if one is to get good information for industrial applications. The ALE formulation is under development and is the most promising for providing a complete numerical simulation.

To shorten computation times and reduce the difficulties linked to remeshing, one can work with separate models for two distinct regions. The first deals with thermal diffusion in the sheets and needs only a coarse spatial resolution. The second model deals with the region near the tool, which must describe correctly contact conditions, large deformation of materials, and stirring. This model can be based on FEM or on more original techniques such as SPH [Tartakovsky et al. 2006] or NEM [Alfaro et al. 2008; 2007]. To couple the two models one can use the Arlequin method originally proposed in Ben Dia 1998 (see also [Rateau 2003; Ben Dia and Rateau 2005]), or a similar technique called bridging [Xiao and Belytschko 2004]. These coupling techniques can be considered adequate for FSW modelling.

Heat sources. In FSW, temperature plays a key role because it controls the mechanical resistance of the material. During the process, heating comes from two sources: friction and plastic work. The first occurs at the interface between the tool and the sheets, whereas the second occurs in the bulk of the material. Temperature is the result of a thermal equilibrium written as

$$\rho\, C_p\, \frac{DT}{Dt} = \operatorname{div}(\lambda\, \operatorname{grad} T) + \dot{Q}, \tag{2-1}$$

where ρ is the material density, C_p the specific heat, T the temperature, D/Dt the particle derivative (material derivative), λ the thermal conductivity, and $\dot{Q}$ the volumetric heat source strength, which we can write as $\dot{Q} = \beta\sigma : \mathrm{D}$, where D is the deformation velocity gradient tensor, σ is the stress tensor, and $\beta = 0.9$.

Q_{surf}, the surface heat source due to friction, appears as a boundary condition in the interface between the tool and the sheet:

$$Q_{\text{surf}} = \lambda\, \operatorname{grad}(T) \cdot n, \tag{2-2}$$

where n is the normal to the surface.

To determine the temperature, three different approaches in the literature can be distinguished, according to the desired objective (heating, material flow, microstructure, residual state, and so on). The differences between these three approaches also come from the level of integration of the process parameters and tool geometry and the calculation time needed. It is always necessary to find a compromise between completeness and computation time.

The first approach consists in using experimental measurements to determine the heat flux by an inverse method. Chao and Qi [1999] and Dickerson et al. [2003] measured temperature using thermocouples to determine the heat flux. Several teams have used torque measurements to determine the power involved in the process and so the heat flux [Dickerson et al. 2003; Shi et al. 2003; Khandkar et al. 2006; Simar et al. 2004; Gallais et al. 2004].

The second approach is based on an analytical formulation of the heat flux

$$Q_{\text{surf}} = \mu F \omega \alpha, \tag{2-3}$$

where Q_{surf} is the heat flux, μ is the friction coefficient between tool and sheet, F is the plunge force, ω is the rotational velocity, and α is a parameter related to the tool geometry.

This equation is then used either in analytical modelling using the Rosenthal equation [Rosenthal and Schmerber 1938; Rosenthal 1941; Feng et al. 1998; Mandal and Williamson 2006], or in finite element simulations using moving sources [Song and Kovacevic 2003b; 2003a; Chen and Kovacevic 2003a].

The last approach tends to calculate the heat flux directly by modelling the mechanical role of the tool and so is clearly more predictive than the first approach. The geometry of the tool and its mechanical interaction with the sheet is then determined by means of finite element simulations [Ulysse 2002; Fourment et al. 2004; Schmidt and Hattel 2004; 2005; Guerdoux and Fourment 2005; Buffa et al. 2006b; 2006a; 2007; Fratini et al. 2007]. The heat generated by friction between tool and sheets is modelled using the classical friction equation

$$Q_{\text{surf}} = \tau v_{\text{s}}, \tag{2-4}$$

relating the tangential stress τ to the sliding velocity v_{s} through the friction parameters.

Clearly the contact conditions are critical for an accurate and realistic determination of the heat flux. If the tangential stress and/or the sliding velocity are not well estimated, the heat flux is not well estimated. The contact surface also plays an important role, because the total flux is given by the integration of (2-4) over the whole surface.

Physical models. In this section, the constitutive equation and friction law commonly used for FSW simulation are discussed.

Constitutive law. During the FSW process, the material is submitted to changes of temperature of a few hundred degrees and to widely varying strain rates. Thus the constitutive equation has to capture the strain-rate- and temperature-dependent behaviour over a large range of these parameters. In addition, the behaviour of the material changes with deformation related to strain hardening and microstructure evolution. In the literature, one can find both very simple and more sophisticated modellings involving microstructural changes, all of them based on a viscoplastic formalism, whether or not using a plastic threshold. For example, the model of [Myhr and Grong 1991a; 1991b] is used in [Bastier et al. 2006; 2008; Feulvarch et al. 2005a; 2005b; 2007; Feulvarch 2006]; it takes into account the dissolution of precipitates due to the temperature evolution in aluminium alloys.

In the viscoplastic formalism, two constitutive equations are more currently used. The first is the Johnson–Cook relation, used for example by Schmidt and Hattel [2004; 2005], which phenomenologically accounts for the strain, strain rate, and temperature dependence of the material behaviour in an uncoupled manner. It is written

$$\sigma_{em} = \left(A + B[\epsilon_{\text{eq}}^{\text{pl}}]^n\right)\left(1 + C \ln \frac{\dot{\epsilon}_{\text{eq}}^{\text{pl}}}{\dot{\epsilon}_0}\right)\left(1 - \left[\frac{T - T_{\text{ref}}}{T_{\text{melt}} - T_{\text{ref}}}\right]^m\right) \tag{2-5}$$

where σ_{eq}, $\epsilon_{\text{eq}}^{\text{pl}}$, $\dot{\epsilon}_{\text{eq}}^{\text{pl}}$, and $\dot{\epsilon}_0$ ($1\ \text{s}^{-1}$) are respectively the equivalent von Mises stress, the equivalent plastic strain, the equivalent plastic strain rate, and the normalising strain rate, while A, B, C, n, T_{melt}, T_{ref}, and m are material constants. The relation captures a plastic threshold and consequently accepts the presence of residual stresses when the strain rate is reduced to zero.

Power law-type constitutive equations such as the Norton–Hoff model are also used [Fourment et al. 2004; Guerdoux and Fourment 2005]. They are currently combined with the Eulerian representation

$$\sigma_{\text{eq}} = 3K\left(\sqrt{3}\dot{\epsilon}_{\text{eq}}\right)^{m-1}\dot{\epsilon}_{\text{eq}}, \tag{2-6}$$

where $K = K_0(\epsilon + \epsilon_0)^n \exp(\beta/T)$ is the consistency, $\dot{\epsilon}_{\text{eq}}$ is the equivalent strain rate, and m, K_0, ϵ_0, n, and β are material constants. Contrary to the Johnson–Cook equation, when the strain rate is reduced to zero, no more stress exists within the material.

Contact law. For friction modelling, only two laws are found in the literature. The first, used mainly in solid mechanics [Xu and Deng 2001; Xu and Deng 2002; 2003; Schmidt and Hattel 2004; 2005], is a modification of Coulomb friction law

$$\tau = \mu p, \tag{2-7}$$

which expresses the tangential stress as a function of the contact pressure p and the friction coefficient μ. It is modified in that the tangential stress is limited to $\tau_{\max}$, a value related to the ultimate tensile strength σ_u by $\tau_{\max} = \sigma_u/\sqrt{3}$; see Figure 4.

The second friction law is the Norton law, currently used in fluid mechanics [Fourment et al. 2004; Guerdoux and Fourment 2005; Feulvarch et al. 2005a; 2005b; 2007; Feulvarch 2006]. It expresses the tangential stress in terms of the friction coefficient μ, the consistency K, and the differential velocity V:

$$\tau = -\mu K |V|^{q-1} V, \tag{2-8}$$

where q is a material constant.

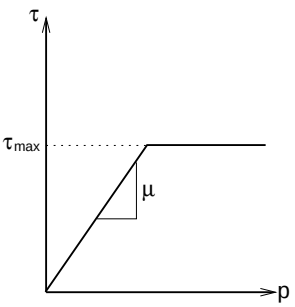

Figure 4. Modified Coulomb friction law.

But the heat partition between sheet and tool is not really justified by the different authors. How much heat is dissipated in the sheet? The only physical consideration used to determine this is the difference in material effusivity of each part. This problem needs to be highlighted because it governs the temperature evolution in the sheet, and so the final result. Moreover, the definition of friction must vary with the velocity and temperature in the transient phase. For the steady state, even if the conditions are known, the friction coefficient must be correctly evaluated.

3. Numerical issues

In addition to the thermomechanical modelling, algorithms have to be chosen to deal with the numerical resolution of the thermal and mechanical equations of the problem. This section considers three numerical issues in ABAQUS/Explicit: contact definition, mass scaling, and ALE use. These aspects are unfortunately not analysed in the literature, although they strongly affect the numerical results.

3.1. ***Contact definition.*** We turn first to the management of contact between sheet and tool, and in particular the contact between shoulder and sheet. Contact problems are among the most delicate modelled in the literature [Kikuchi 1982; Alart and Curnier 1991; Fortin and Glowinski 1983; Perić and Owen 1992; Simo and Laursen 1992; Wriggers 1995; Papadopoulos and Solberg 1998; Aggoune et al. 2006].

ABAQUS offers two main approaches for unilateral contact. The first is based on a hard contact definition and uses a Lagrange multiplier, representing the contact pressure, to enforce the contact constraint. The second is based on a softened contact definition, postulating a regular relation between the contact pressure and the overclosure between the master and slave surfaces.

Here we focus on the second approach, and ask whether the friction coefficient imposed in the input file of ABAQUS/Explicit is respected. Only the interaction between the shoulder and the sheets is considered; the interface between the pin and the sheet is not modelled, to uncouple the roles of each part of the tool. The master surface is the tool, which is considered undeformable, and the slave surface is the sheet.

For the slave surface definition, two choices are offered by ABAQUS/Explicit: node-based, where the contact forces are considered directly at the nodes, or element-based, where the reactions are calculated on the surface of the elements. ABAQUS/Explicit warns that "a node-based surface should be used with caution or not at all if accurate contact stresses are needed or if heat will be exchanged between the two surfaces" [ABAQUS 2006]. To explore this recommendation more precisely, numerical computations were performed using these two choices, as follows. The friction law is considered without the limitation of the equivalent friction stress. The dwelling phase, where the tool is in contact with the sheets and rotates around its own axis, is simulated. The friction coefficient is then postcalculated from the computed stresses and must be compared with the coefficient imposed in the input file ($\mu = 0.3$):

$$\mu = \frac{\tau_{\text{eq}}}{\sigma_{33}}, \tag{3-1}$$

where $\tau_{\text{eq}} = \sqrt{\sigma_{13}^2 + \sigma_{23}^2}$ is the equivalent friction stress and σ_{33} is the normal stress (the index 3 corresponds to the normal to the contact surface).

Figure 5 presents the postcalculated friction coefficient μ for four different elements, sketched in white, in contact with the shoulder. It reveals that the element based definition allows μ to be closer to the prescribed friction coefficient than the node based definition even though the value is not exactly the one imposed in the input file. This confirms the ABAQUS/Explicit recommendation.

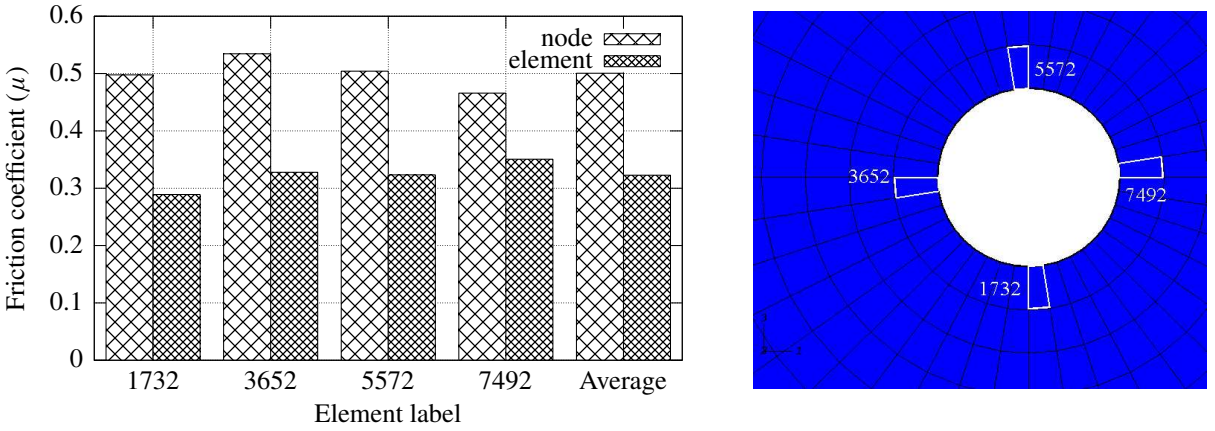

Figure 5. Friction coefficient (left) calculated using node-based and element-based surfaces, for the four elements highlighted on the right.

3.2. ***Mass scaling influence.*** In a FEM, the dynamic problem is written for each node of the mesh as

$$P - I = M\ddot{u}, \tag{3-2}$$

where P, I, M, and $\ddot{u}$ represent respectively the applied forces, the internal forces, the mass matrix, and the node acceleration.

ABAQUS/Explicit solves the equilibrium (3-2) by an explicit algorithm. The acceleration of each node is determined as a function of its mass and forces applied to it:

$$\ddot{u}|_t = M^{-1}(P - I)|_t. \tag{3-3}$$

The mass matrix used in this formulation is diagonal, which simplifies the explicit calculation. The node velocities at time $(t + \Delta t/2)$ are determined by

$$\dot{u}|_{t+\Delta t/2} = \dot{u}|_{t-\Delta t/2} + \frac{\Delta t|_{t+\Delta t} + \Delta t|_t}{2}\,\ddot{u}|_t. \tag{3-4}$$

Then, the displacements of nodes are determined by

$$u|_{t+\Delta t} = u|_t + \Delta t|_{t+\Delta t}\,\dot{u}|_{t+\Delta t/2}. \tag{3-5}$$

As shown by equations (3-3), (3-4) and (3-5), the dynamic computation in ABAQUS/Explicit does not need a stiffness matrix decomposition. The solutions are given at the end of the time increment without any iteration. So each increment needs little CPU time. However, the algorithm has a time cost related to the mesh size. In fact, the time increment (Δt) must be less than a certain limit, to ensure the stability of the calculation and avoid fluctuations in the solution. This limit is the smallest time needed for an elastic wave to propagate through a mesh element [Schmidt and Hattel 2005; ABAQUS 2006; Liu 2006; Wang et al. 2007]:

$$\Delta t = \frac{L_e}{C_d}, \tag{3-6}$$

where L_e is the length of the smallest mesh element and C_d is the celerity of elastic waves through the element considered. For a solid in an elastic regime, we have

$$C_d = \sqrt{\frac{E}{\rho}}, \tag{3-7}$$

where E is the Young's modulus and ρ the mass density of the material. Therefore, once the mesh is determined, the simulation time is proportional to the real duration of the process to be simulated.

To reduce computation time without increasing the element size (which would compromise the simulation quality at the contact surface), one can increase artificially the value of the density ρ, and so also, according to (3-6) and (3-7), the value of Δt. This technique is known as mass scaling, and it used also in other explicit software such as LS-DYNA [Liu 2006; Wang et al. 2007] and METAFOR [Papeleux and Ponthot 2002].

To analyse the effect of mass scaling, we compared the friction coefficient obtained using four different time increments in the previously described simulations. (The increment time was selected directly, and ABAQUS/Explicit determines the corresponding mass factor.) Figure 6 shows the results obtained for the same elements used in Figure 5. Clearly, for a high value of mass scaling (n_3 and e_3), fluctuations are important and the results are not physically acceptable, since the calculated friction coefficient is higher than 1. With less drastic mass scaling, the element-based friction coefficient displays a smaller dependence on mass scaling than the node-based one. This again confirms the ABAQUS/Explicit recommendation, and the element-based surface was chosen in further simulations.

3.3. ***ALE in ABAQUS/Explicit.*** Since large deformations occur during the process, mesh distortions appear quickly in a Lagrangian finite element simulation. ABAQUS/Explicit offers an adaptive meshing mode called ALE [Song and Kovacevic 2003b; 2003a; Schmidt and Hattel 2004; 2005; Zhang et al. 2005; 2007] which repositions nodes with no change in the number or connectivity of elements. Figure

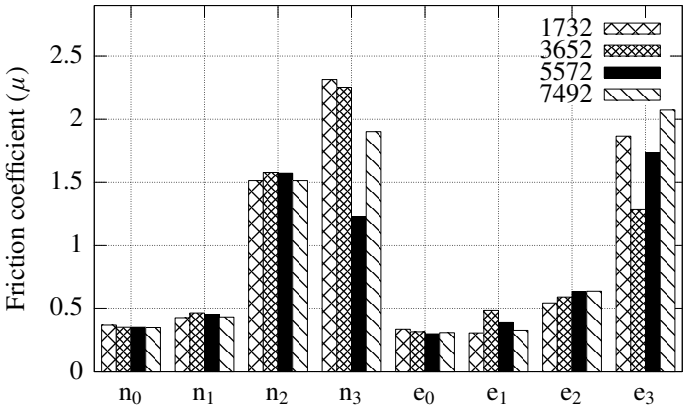

Figure 6. Influence of mass scaling on the calculated friction coefficient. Notation: "n" and "e" stand for node- and element-based surfaces; the subscripts indicate increasingly more drastic mass scaling (0 corresponds to $\Delta t = 0.00008$, or no mass scaling, while 1, 2 and 3 correspond to $\Delta t = 0.0001$, 0.0005, and 0.001, respectively).

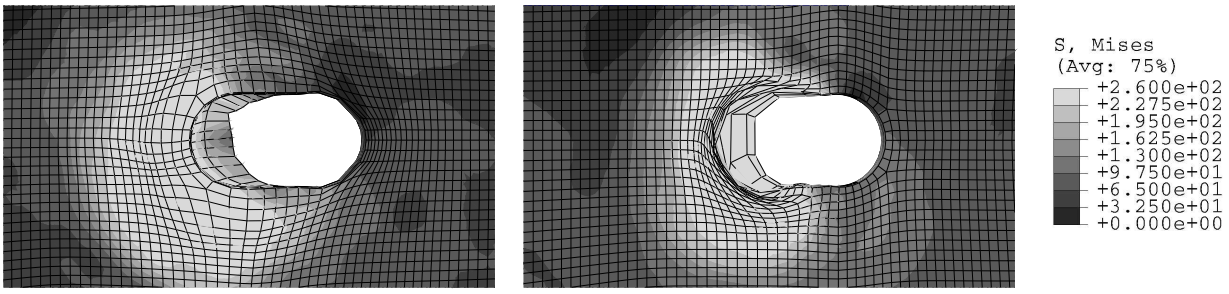

Figure 7. Von Mises stress distribution after a 5 mm translation with adaptive meshing (left) and without it (right).

7 shows the von Mises stress distribution obtained with and without the adaptive meshing for a pure elastoplastic simulation where the tool undergoes a 5 mm translation. The distortions clearly decrease but do not vanish when the ALE method is used. The element in contact with the tool gets thinner and thinner due to the adaptive meshing and finally the small thickness of the elements makes the calculation diverge.

Two parameters must be chosen to perform the adaptive meshing: the frequency of node repositioning and the number of mesh sweeps (the number of times the algorithm is used). Their values have to be high enough to avoid distortions, but not so high as to degrade the information excessively. (When nodes are moved during each sweep, the fields must be transferred to the new mesh, leading to a loss of information due to interpolation.)

4. Numerical analysis

The preceding analysis can be of help in making certain modelling and numerical choices for FSW simulations. Ultimately, a systematic exploration of such choices can clarify how the temperature field is influenced by process parameters such as the plunge force or the translation and rotation speeds of the tool. The results presented here are the first ones obtained after having chosen the parameters presented in earlier sections.

Material and geometry. The tool is considered analytically rigid, which means in ABAQUS/Explicit terminology undeformable and isothermal. It is made of two simple cylinders: an inferior rounded one for the pin, with radius $r_p = 2.5$ mm and height $h_p = 3$ mm, and an upper one for the shoulder, with radius $r_e = 6.5$ mm and height $h_e = 5$ mm as illustrated in Figure 8.

The sheet is modelled by the extrusion of a square of length $L_s = 40$ mm with a hole in the center of diameter $D_s = 5$ mm and thickness $E_s = 4$ mm. The anvil is also modelled by the extrusion of the same square (without the hole) with thickness $E_a = 5$ mm.

The sheet is made of aluminium 2024-T3. The Johnson–Cook constitutive equation, (2-5), is chosen, using the following parameters, taken from [Schmidt and Hattel 2004; 2005]:

$$A = 369\,\text{MPa}, \quad C = 0.0083, \quad T_{\text{melt}} = 502^\circ\text{C}, \quad m = 1.7,$$
$$B = 684\,\text{MPa}, \quad T_{\text{ref}} = 25^\circ\text{C}, \quad n = 0.73.$$

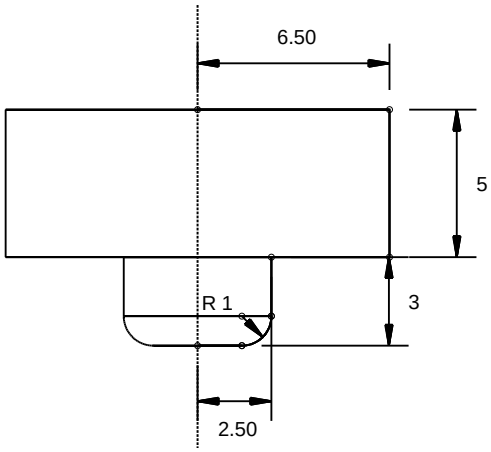

Figure 8. Tool used for simulations (dimensions in mm).

The tool and the anvil are made of classical steel. The physical properties (material conductivity λ, specific heat C_p, and density ρ) used for aluminium and steel are as follows:

	λ (W m^{-1} K^{-1})	C_p (J kg^{-1} K^{-1})	ρ (kg m^{-3})
Aluminium	140	920	2780
Steel	36	450	7800

Based on experimental observations, the constitutive equation for the anvil is limited to linear elasticity (using a Young's modulus of 2.1×10^5 MPa and a Poisson's ratio of 0.3) in order to decrease computation time and because only the behaviour of the sheet is being studied.

The process is decomposed into three steps, presented in Figure 9:

(1) Plunge (preexisting hole, 1 s): the tool is in contact with the sheet; a force $F = 1200$ N orthogonal to the sheet is applied to the tool.

(2) Dwelling (beginning of tool rotation, 2 s): an additional angular velocity $\omega = 42$ rad/s is imposed on the tool.

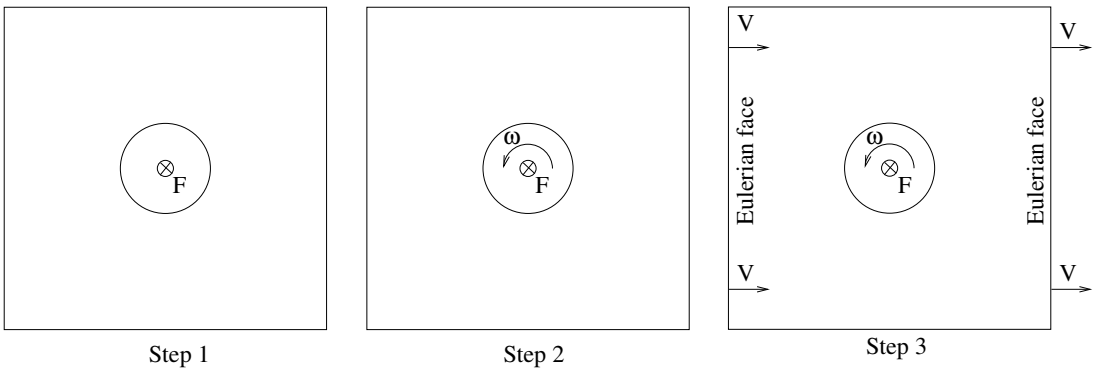

Figure 9. Boundary conditions of each step.

(3) Translation (10 s): Eulerian faces are used to simulate the material flow in the sheet; material flows through these faces with velocity $V = 0.5$ mm/s. This choice is helpful in decreasing mesh distortion.

Adaptive meshing is used only in steps 2 and 3, and is applied to the entire sheet with frequency 1 (at the end of each increment); the number of sweeps is 10. These parameters are chosen from the optimization study performed previously.

The definition of the slave surface of the contact between tool and sheet is element based as justified in Section 3.1.

For these simulations, about 50000 hexahedral elements with reduced integration (C3D8RT) were used, and the computation time varied between 3 and 19 hours. The translation step accounts for most of the CPU time overall.

Temperature results. As discussed, the use of mass scaling can decrease computation time but may lead to loss of precision and hence predictability. Here we consider the effect of mass scaling on the calculated temperature field. We chose three elements on the sheet, shown in Figure 10: element A is under the shoulder and in contact with the pin; element B lies under the shoulder, 6 mm from the centre of the sheet; and element C is 9.5 mm away from the centre of the sheet.

Figure 11 shows the calculated temperature evolution at these elements. The same values of Δt are used as in Figure 6, reflecting increasingly drastic mass scaling. First, the temperature found is of the same order as the experimental one observed in the test using conditions close to the numerical simulation. The parameters are taken from the literature and consequently are not fitted to match experimental results. Second, for elements A and B, fluctuations clearly appear for the whole simulation. This phenomenon is magnified with the use of mass scaling. For element A, the mass scaling leads to an underestimation of the temperature value, and for element B to an overestimation. Thus mass scaling can cause errors in either direction in the calculation of temperature. For element C, which is far from the tool, there is no fluctuation and mass scaling has only a weak influence. So the overall heating due to the tool is well predicted but local results fluctuate and are not really accurate because mass scaling has an effect on the management of the contact.

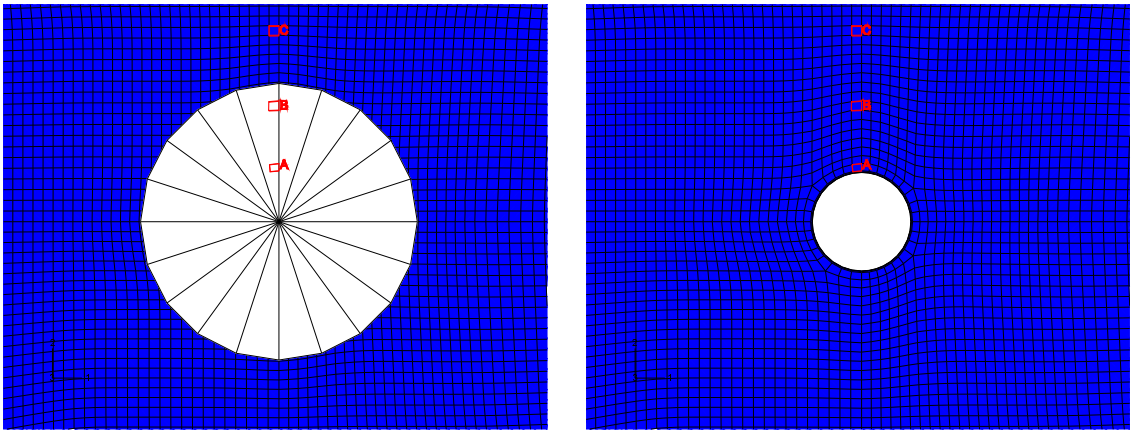

Figure 10. Position of elements in the sheet for the complete simulation.

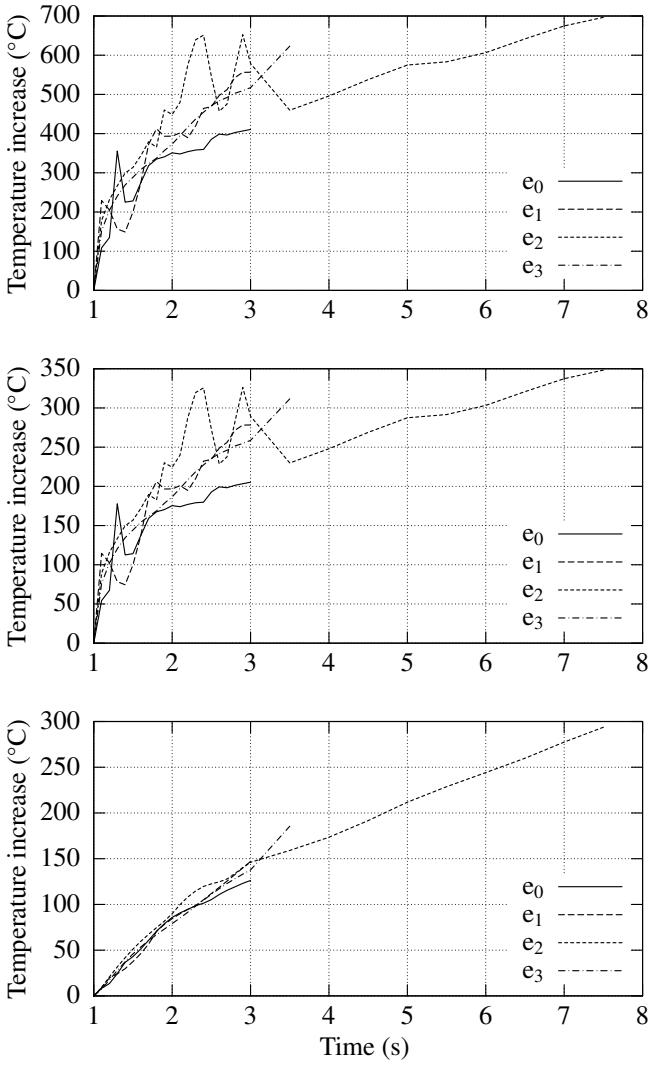

Figure 11. Increase in temperature for elements A (top), B (center), and C (bottom); simulation using element-based surfaces with Δt equal to 0.00008 (e_0), 0.0001 (e_1), 0.0005 (e_2), and 0.001 (e_3). The time scale begins at 1 s because step 1 is omitted.

Material flow results. Understanding and controlling the material flow are crucial to the success of the FSW process, are closely related to the temperature field. In view of the link between microstructure evolution and the strain path of the particle [Xu and Deng 2003; Schmidt and Hattel 2004], we also study the latter: Figure 12 shows the von Mises equivalent plastic strain partition in a cut perpendicular to the welding direction. We can clearly associate the zone of highest equivalent plastic strain with the thermomechanical affected zone (TMAZ). The vase shape of the TMAZ and the lack of symmetry between the advancing and retreating sides are in good agreement with experimental observations and numerical simulations found in [Xu and Deng 2003; Schmidt and Hattel 2004; Mishra and Ma 2005]. We notice the presence of a highly deformed zone at the center of the TMAZ, corresponding to the nugget.

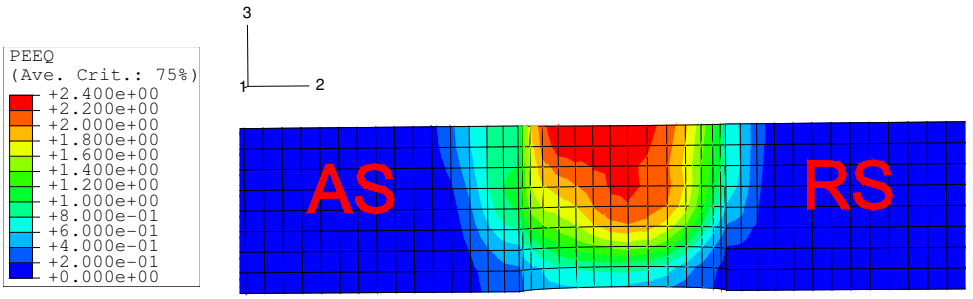

Figure 12. Cross-section of the weld: von Mises equivalent plastic strain partition. AS is the advancing side, RS the retreating side.

Figure 13 shows the results concerning the elements near the pin for different sections through the sheet, perpendicular to the axis of the tool. The results come from an analytical calculation in which the particle velocities are imposed on the contact surface and depend on the advancing speed, the angular velocity, and the pitch of the pin.

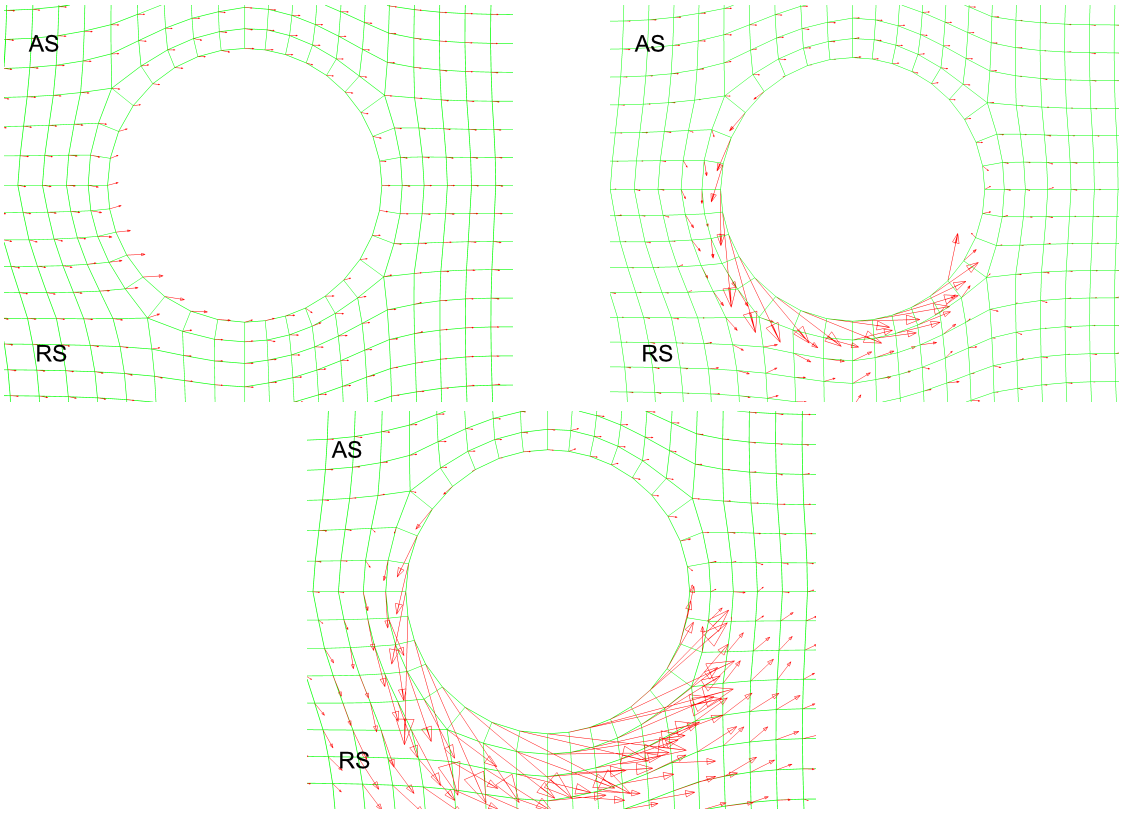

Figure 13. Calculated angular velocity and flow velocity: under the shoulder (top left), mid thickness (top right), and at the bottom of the weld (bottom). For each figure, the advancing side is at the top and the retreating side is at the bottom.

The results agree qualitatively with those in [Nandan et al. 2007]; see especially Figure 15 there, showing how that material moves from the advancing side to the retreating side. This observation was made using thin copper sheets as material markers. Quantitatively, our simulation results obtained are close to those of Nandan et al. for the upper part of the weld (contact with the shoulder), except near the tool on the advancing side where the material flow does not follow the movement of the tool. In addition, in the bottom part of the weld the rotational motion of the pin does not affect the material flow. It is similar to a flow around a fixed obstacle that does not stick to it. This phenomenon may come from a too low normal stress at the pin/sheet interface, which does not provide high enough tangential stress. In the upper part, the normal force is imposed on the tool and stirs the material. Note that a hole is still present behind the tool, even though a small amount of material seems to be stirred behind the tool.

5. Conclusion

We have examined different approaches used in the literature and based on commercial codes to simulate the FSW process, highlighting their strengths and weaknesses. The choice of an approach is motivated by the desired predictive feature for the simulation.

From the viewpoint of kinematics, the ALE representation seems to be the most promising method to reduce mesh distortions; it does not prevent computationally expensive remeshing but reduces it.

One way to reduce computation time is to use mass scaling. However, excessive mass scaling can degrade the quality of the outputs. The technique of coupling two different models seems to provide a good compromise, since it allows us to largely reduce or avoid remeshing.

For the model to be predictive, material mixing must be well described in order to predict defects like void formation in the weld joint. This is possible if the complex geometry of the pin and the shoulder is considered in the simulation.

References

[ABAQUS 2006] *ABAQUS user's manual*, Hibbitt, Karlsson and Sorensen, Pawtucket, RI, 2006.

[Aggoune et al. 2006] W. Aggoune, H. Zahrouni, and M. Potier-Ferry, "Asymptotic numerical methods for unilateral contact", *Int. J. Numer. Methods Eng.* **68**:6 (2006), 605–631.

[Alart and Curnier 1991] P. Alart and A. Curnier, "A mixed formulation for frictional contact problems prone to Newton like solution methods", *Comput. Methods Appl. Mech. Eng.* **92**:3 (1991), 353–375.

[Alfaro et al. 2007] I. Alfaro, L. Fratini, E. Cueto, F. Chinesta, and F. Micari, "Meshless simulation of friction stir welding", pp. 203–208 in *Materials processing and design: modeling, simulation and applications: NUMIFORM '07* (Porto, 2007), edited by J. M. A. César de Sá and A. D. Santos, AIP Conference Proceedings **908**, American Inst. of Physics, Melville, NY, 2007.

[Alfaro et al. 2008] I. Alfaro, L. Fratini, E. Cueto, and F. Chinesta, "Numerical simulation of friction stir welding by natural element methods", *Int. J. Mater. Form.* Supplement 1 (2008), 1079–1082.

[Askes and Sluys 2000] H. Askes and L. J. Sluys, "Remeshing strategies for adaptive ALE analysis of strain localisation", *Eur. J. Mech. A Solids* **19**:3 (2000), 447–467.

[Aymone et al. 2001] J. L. F. Aymone, E. Bittencourt, and G. J. Creus, "Simulation of 3D metal-forming using an arbitrary Lagrangian–Eulerian finite element method", *J. Mater. Process. Technol.* **110**:2 (2001), 218–232.

[Bastier 2006] A. Bastier, *Modélisation du soudage d'alliages d'aluminium par friction et malaxage*, Ph.D. thesis, École Polytechnique, Palaiseau, 2006, Available at http://pastel.paristech.org/2089.

[Bastier et al. 2006] A. Bastier, M. H. Maitournam, K. Dang Van, and F. Roger, "Steady state thermomechanical modelling of friction stir welding", *Sci. Technol. Weld. Joi.* **11**:3 (2006), 278–288.

[Bastier et al. 2008] A. Bastier, M. H. Maitournam, F. Roger, and K. Dang Van, "Modelling of the residual state of friction stir welded plates", *J. Mater. Process. Technol.* **200**:1–3 (2008), 25–37.

[Ben Dia 1998] H. Ben Dia, "Multiscale mechanical problems: the Arlequin method", *C. R. Acad. Sci. II B Mec.* **326** (1998), 899–904.

[Ben Dia and Rateau 2005] H. Ben Dia and G. Rateau, "The Arlequin method as a flexible engineering design tool", *Int. J. Numer. Methods Eng.* **62**:11 (2005), 1442–1462.

[Buffa et al. 2006a] G. Buffa, J. Hua, R. Shivpuri, and L. Fratini, "Design of the friction stir welding tool using the continuum based FEM model", *Mater. Sci. Eng. A* **419**:1–2 (2006), 381–388.

[Buffa et al. 2006b] G. Buffa, J. Hua, R. Shivpuri, and L. Fratini, "A continuum based FEM model for friction stir welding: model development", *Mater. Sci. Eng. A* **419**:1–2 (2006), 389–396.

[Buffa et al. 2007] G. Buffa, L. Fratini, and R. Shivpuri, "CDRX modelling in friction stir welding of AA7075-T6 aluminum alloy: analytical approaches", *J. Mater. Process. Technol.* **191**:1–3 (2007), 356–359.

[Chao and Qi 1999] Y. J. Chao and X. Qi, "Heat transfer and thermo-mechanical analysis of friction stir joining of AA6061-T6 plates", in *1st International Symposium on Friction Stir Welding* (Thousand Oaks, CA, 1999), TWI, Cambridge, 1999.

[Chen and Kovacevic 2003a] C. Chen and R. Kovacevic, "Finite element modelling of thermomechanical performance of friction stir welding", in *4th International Symposium on Friction Stir Welding* (Park City, UT, 2003), TWI, Cambridge, 2003.

[Chen and Kovacevic 2003b] C. M. Chen and R. Kovacevic, "Finite element modeling of friction stir welding: thermal and thermomechanical analysis", *Int. J. Mach. Tool. Manuf.* **43**:13 (2003), 1319–1326.

[Colegrove and Shercliff 2004] P. A. Colegrove and H. R. Shercliff, "Modelling the friction stir welding of aerospace alloys", in *5th International Symposium on Friction Stir Welding* (Metz, 2004), TWI, Cambridge, 2004.

[Colegrove and Shercliff 2005] P. A. Colegrove and H. R. Shercliff, "3-Dimensional CFD modelling of flow round a threaded friction stir welding tool profile", *J. Mater. Process. Technol.* **169**:2 (2005), 320–327.

[Colegrove and Shercliff 2006] P. A. Colegrove and H. R. Shercliff, "CFD modelling of friction stir welding of thick plate 7449 aluminium alloy", *Sci. Technol. Weld. Joi.* **11**:4 (2006), 429–441.

[Colegrove et al. 2000] P. A. Colegrove, M. Painter, D. Graham, and T. Miller, "3-dimensional flow and thermal modelling of the friction stir welding process", in *2nd International Symposium on Friction Stir Welding* (Gothenborg, 2000), TWI, Cambridge, 2000.

[Colegrove et al. 2003] P. A. Colegrove, H. R. Shercliff, and P. L. Threadgill, "Modelling and development of the Trivex friction stir welding tool", in *4th International Symposium on Friction Stir Welding* (Park City, UT, 2003), TWI, Cambridge, 2003.

[Dickerson et al. 2003] T. L. Dickerson, Q.-Y. Shi, and H. R. Shercliff, "Heat flow into friction stir welding tools", in *4th International Symposium on Friction Stir Welding* (Park City, UT, 2003), TWI, Cambridge, 2003.

[Feng et al. 1998] Z. Feng, J. E. Gould, and T. J. Lienert, "A heat flow model for friction stir welding of aluminium alloys", pp. 149–158 in *Hot deformation of aluminum alloys II: proceedings of the Second Symposium held at the 1998 TMS Fall Meeting* (Rosemont, IL, 1998), edited by T. R. Bieler et al., TMS, Warrendale, PA, 1998.

[Feulvarch 2006] E. Feulvarch, *Modélisation numérique du soudage par friction-malaxage (friction stir welding)*, Ph.D. thesis, Université Jean Monnet, Saint-Etienne, 2006.

[Feulvarch et al. 2005a] E. Feulvarch, F. Boitout, and J.-M. Bergheau, "Friction stir welding: modélisation de l'écoulement de la matière pendant la phase de soudage", in *17ème Congrès Français de Mécanique* (Troyes, 2005), Université Technologie de Troyes, Troyes, 2005.

[Feulvarch et al. 2005b] E. Feulvarch, F. Boitout, and J.-M. Bergheau, "Modélisation thermomécanique et microstructurale du soudage par friction-malaxage (friction stir welding): développement d'un modèle élément fini", pp. 347–352 in *Septième Colloque National en Calcul des Structures* (Giens, 2005), vol. 2, edited by R. Ohayon et al., Hermes Science/Lavoisier, Paris, 2005.

[Feulvarch et al. 2007] E. Feulvarch, V. Robin, F. Boitout, and J.-M. Bergheau, "A 3D finite element modelling for thermofluid flow in friction stir welding", pp. 711–724 in *Mathematical modelling of weld phenomena* (Graz, 2006), vol. 8, edited by H. Cerjak et al., Verlag der Technischen Universität Graz, Graz, 2007.

[Fortin and Glowinski 1983] M. Fortin and R. Glowinski, *Augmented Lagrangian methods: applications to the numerical solutions of boundary-value problems*, Studies in Mathematics and its Applications **15**, North-Holland, Amsterdam, 1983.

[Fourment et al. 2004] L. Fourment, S. Guerdoux, M. Miles, and T. Nelson, "Numerical simulation of the friction stir welding process using both Lagrangian and arbitrary Lagrangian Eulerian formulations", in *5th International Symposium on Friction Stir Welding* (Metz, 2004), TWI, Cambridge, 2004.

[Fratini et al. 2007] L. Fratini, G. Buffa, and R. Shivpuri, "Improving friction stir welding of blanks of different thicknesses", *Mater. Sci. Eng. A* **459**:1–2 (2007), 209–215.

[Gadala 2004] M. S. Gadala, "Recent trends in ALE formulation and its applications in solid mechanics", *Comput. Methods Appl. Mech. Eng.* **193**:39–41 (2004), 4247–4275.

[Gadala et al. 2002] M. S. Gadala, M. R. Movahhedy, and J. Wang, "On the mesh motion for ALE modeling of metal forming processes", *Finite Elem. Anal. Des.* **38**:5 (2002), 435–459.

[Gallais et al. 2004] C. Gallais, A. Denquin, A. Pic, A. Simar, T. Pardoen, and Y. Brechet, "Modelling the relationship between process parameters, microstructural evolutions and mechanical behaviour in a friction stir welded 6xxx aluminium alloy", in *5th International Symposium on Friction Stir Welding* (Metz, 2004), TWI, Cambridge, 2004.

[Guerdoux and Fourment 2005] S. Guerdoux and L. Fourment, "ALE formulation for the numerical simulation of friction stir welding", in *Computational plasticity: fundamentals and applications: proceedings of the Eighth International Conference on Computational Plasticity, COMPLAS VIII* (Barcelona, 2005), edited by E. Oñate et al., CIMNE, Barcelona, 2005. Extended abstract available at http://congress.cimne.upc.es/complas05/admin/Files/FilePaper/p50.pdf.

[Khandkar et al. 2006] M. Z. H. Khandkar, J. A. Khan, A. P. Reynolds, and M. A. Sutton, "Predicting residual thermal stresses in friction stir welded metals", *J. Mater. Process. Technol.* **174**:1–3 (2006), 195–203.

[Kikuchi 1982] N. Kikuchi, "A smoothing technique for reduced integration penalty methods in contact problems", *Int. J. Numer. Methods Eng.* **18**:3 (1982), 343–350.

[Liu 2006] C.-H. Liu, "The simulation of the multi-pass and die-less spinning process", *J. Mater. Process. Technol.* **192-193** (2006), 518–524.

[Mandal and Williamson 2006] S. Mandal and K. Williamson, "A thermomechanical hot channel approach for friction stir welding", *J. Mater. Process. Technol.* **174**:1–3 (2006), 190–194.

[Mishra and Ma 2005] R. S. Mishra and Z. Y. Ma, "Friction stir welding and processing", *Mater. Sci. Eng. R* **50**:1–2 (2005), 1–78.

[Myhr and Grong 1991a] O. R. Myhr and Ø. Grong, "Process modelling applied to 6082-T6 aluminium weldments, 1: Reaction kinetics", *Acta Metall. Mater.* **39**:11 (1991), 2693–2702.

[Myhr and Grong 1991b] O. R. Myhr and Ø. Grong, "Process modelling applied to 6082-T6 aluminium weldments, 2: Applications of model", *Acta Metall. Mater.* **39**:11 (1991), 2703–2708.

[Nandan et al. 2007] R. Nandan, G. G. Roy, T. J. Lienert, and T. Debroy, "Three-dimensional heat and material flow during friction stir welding of mild steel", *Acta Mater.* **55**:3 (2007), 883–895.

[Papadopoulos and Solberg 1998] P. Papadopoulos and J. M. Solberg, "A Lagrange multiplier for the finite element solution of frictionless contact problems", *Math. Comput. Model.* **28**:4–8 (1998), 373–384.

[Papeleux and Ponthot 2002] L. Papeleux and J.-P. Ponthot, "Finite element simulation of springback in sheet metal forming", *J. Mater. Process. Technol.* **125-126** (2002), 785–791.

[Perić and Owen 1992] D. Perić and D. R. J. Owen, "Computational model for 3-D contact problems with friction based on the penalty method", *Int. J. Numer. Methods Eng.* **35**:6 (1992), 1289–1309.

[Rateau 2003] G. Rateau, *Méthode Arlequin pour les problèmes mécaniques multi-échelles: applications à des problèmes de jonction et de fissuration de structures élancées*, Ph.D. thesis, École Centrale Paris, 2003.

[Rosenthal 1941] D. Rosenthal, "Mathematical theory of heat distribution during welding and cutting", *Weld. J.* **20**:5 (1941), 220s–234s.

[Rosenthal and Schmerber 1938] D. Rosenthal and R. Schmerber, "Thermal study of arc welding", *Weld. J.* **17** (1938).

[Schmidt and Hattel 2004] H. Schmidt and J. Hattel, "Modelling thermomechanical conditions at the tool/matrix interface in friction stir welding", in *5th International Symposium on Friction Stir Welding* (Metz, 2004), TWI, Cambridge, 2004.

[Schmidt and Hattel 2005] H. Schmidt and J. Hattel, "A local model for the thermomechanical conditions in friction stir welding", *Model. Simul. Mater. Sci. Eng.* **13**:1 (2005), 77–93.

[Seidel and Reynolds 2003] T. U. Seidel and A. P. Reynolds, "Two-dimensional friction stir welding process model based on fluid mechanics", *Sci. Technol. Weld. Joi.* **8**:3 (2003), 175–183.

[Shi et al. 2003] Q. Shi, T. Dickerson, and H. R. Shercliff, "Thermomechanical FE modelling of friction stir welding of Al-2024 including tool loads", in *4th International Symposium on Friction Stir Welding* (Park City, UT, 2003), TWI, Cambridge, 2003.

[Simar et al. 2004] A. Simar, T. Pardoen, and B. de Meester, "Influence of friction stir welding parameters on the power input and temperature distribution in aluminium alloys", in *5th International Symposium on Friction Stir Welding* (Metz, 2004), TWI, Cambridge, 2004.

[Simo and Laursen 1992] J. C. Simo and T. A. Laursen, "An augmented Lagrangian treatment of contact problems involving friction", *Comput. Struct.* **42**:1 (1992), 97–116.

[Song and Kovacevic 2003a] M. Song and R. Kovacevic, "A coupled heat transfer model for workpiece and tool in friction stir welding", in *4th International Symposium on Friction Stir Welding* (Park City, UT, 2003), TWI, Cambridge, 2003.

[Song and Kovacevic 2003b] M. Song and R. Kovacevic, "Thermal modeling of friction stir welding in a moving coordinate system and its validation", *Int. J. Mach. Tool. Manuf.* **43**:6 (2003), 605–615.

[Tartakovsky et al. 2006] A. M. Tartakovsky, G. J. Grant, X. Sun, and M. A. Khaleel, "Modeling of friction stir welding (FSW) process with smooth particle hydrodynamics (SPH)", in *Welding & joining & fastening & friction stir welding* (Detroit, MI, 2006), Society of Automotive Engineers, Warrendale, PA, 2006. Paper # 2006-01-1394.

[Ulysse 2002] P. Ulysse, "Three-dimentional modeling of the friction stir-welding process", *Int. J. Mach. Tool. Manuf.* **42**:14 (2002), 1549–1557.

[Wang et al. 2007] Z. W. Wang, S. Q. Zeng, X. H. Yang, and C. Cheng, "The key technology and realization of virtual ring rolling", *J. Mater. Process. Technol.* **182**:1–3 (2007), 374–381.

[Wriggers 1995] P. Wriggers, "Finite element algorithms for contact problems", *Arch. Comput. Methods Eng.* **2**:4 (1995), 1–49.

[Xiao and Belytschko 2004] S. P. Xiao and T. Belytschko, "A bridging domain method for coupling continua with molecular dynamics", *Comput. Methods Appl. Mech. Eng.* **193**:17–20 (2004), 1645–1669.

[Xu and Deng 2001] S. Xu and X. Deng, "Solid mechanics simulation of friction stir welding process", pp. 631–638 in *Transactions of NAMRI/SME* (Gainesville, FL, 2001), vol. XXIX, Society of Manufacturing Engineers, Dearborn, MI, 2001.

[Xu and Deng 2002] S. Xu and X. Deng, "A three-dimensional model for the friction-stir welding process", pp. 699–704 in *Developments in theoretical and applied mechanics* (*SECTAM XXI*) (Orlando, FL, 2002), edited by A. Kassab and H. Mahfuz, Rivercross, Orlando, FL, 2002. Paper # 2108.

[Xu and Deng 2003] S. Xu and X. Deng, "Two and three dimensional finite element models for the friction stir welding process", in *4th International Symposium on Friction Stir Welding* (Park City, UT, 2003), TWI, Cambridge, 2003.

[Zhang et al. 2005] H. W. Zhang, Z. Zhang, and J. T. Chen, "The finite element simulation of the friction stir welding process", *Mater. Sci. Eng. A* **403**:1–2 (2005), 340–348.

[Zhang et al. 2007] H. W. Zhang, Z. Zhang, and J. T. Chen, "3D modeling of material flow in friction stir welding under different process parameters", *J. Mater. Process. Technol.* **183**:1 (2007), 62–70.

Received 17 Dec 2007. Revised 12 Dec 2008. Accepted 15 Dec 2008.

OLIVIER LORRAIN: olivier.lorrain@metz.ensam.fr
LPMM UMR CNRS 7554, Arts et Métiers ParisTech Metz, 4 Rue Augustin Fresnel, 57078 Metz, France

JÉRÔME SERRI: serri@lpmm.sciences.univ-metz.fr
LRMA-LE2I/UFR Sciences & Techniques, Antenne d'Auxerre, Route des Plaines de l'Yonne, BP16, 89010 Auxerre, France

VÉRONIQUE FAVIER: veronique.favier@paris.ensam.fr
LIM UMR CNRS 8006, Arts et Métiers ParisTech Paris, 151 Boulevard de l'Hôpital, 75013 Paris, France

HAMID ZAHROUNI: zahrouni@univ-metz.fr
LPMM UMR CNRS 7554, Université de Metz, Ile du Saulcy, 57045 Metz, France

MOURAD EL HADROUZ: mourad.elhadrouz@metz.ensam.fr
LPMM UMR CNRS 7554, Arts et Métiers ParisTech Metz, 4 Rue Augustin Fresnel, 57078 Metz, France